Reliability Engineering and System Safety 94 (2009) 1718–1728

Contents lists available at ScienceDirect

Reliability Engineering and System Safety

journal homepage: www.elsevier.com/locate/ress

Satellite and satellite subsystems reliability: Statistical data analysis and modeling

Jean-Francois Castet, Joseph H. Saleh *

School of Aerospace Engineering, Georgia Institute of Technology, 270 Ferst Drive, Atlanta, GA 30332-0150, USA

ARTICLE INFO

Article history:
Received 26 March 2009
Received in revised form
1 May 2009
Accepted 13 May 2009
Available online 20 May 2009

Keywords:
Reliability
Satellite
Satellite subsystem
Statistical analysis
Weibull distribution
Maximum likelihood estimation

ABSTRACT

Reliability has long been recognized as a critical attribute for space systems. Unfortunately, limited on-orbit failure data and statistical analyses of satellite reliability exist in the literature. To fill this gap, we recently conducted a nonparametric analysis of satellite reliability for 1584 Earth-orbiting satellites launched between January 1990 and October 2008. In this paper, we extend our statistical analysis of satellite reliability and investigate satellite subsystems reliability. Because our dataset is censored, we make extensive use of the Kaplan–Meier estimator for calculating the reliability functions. We derive confidence intervals for the nonparametric reliability results for each subsystem and conduct parametric fits with Weibull distributions using the maximum likelihood estimation (MLE) approach. We finally conduct a comparative analysis of subsystems failure, identifying the "culprit subsystems" that drive satellite unreliability. The results here presented should prove particularly useful to the space industry for example in redesigning subsystem test and screening programs, or providing an empirical basis for redundancy allocation.

1. Introduction

Reliability has long been recognized as a critical attribute for space systems and an essential metric in spacecraft design and optimization. For example, higher spacecraft reliability may be "purchased" by better, more reliable parts, by subsystem redundancy, or by more extensive testing and screening prior to launch. Unfortunately, despite the recognition of its importance, limited on-orbit failure data and statistical analyses of satellite reliability exist in the technical literature. As a result, inconsistencies persist in the literature due to the absence of an empirical basis for settling the issues, for example, regarding the existence or not of satellite infant mortality. On the one hand, Weibull distributions with a shape parameter around 1.7, "a value commonly used for satellite systems," are typically used to model satellite reliability [1,2]. Recall that a Weibull shape parameter greater than one represents an increasing failure rate or "wear-out" failures but no infant mortality. On the other hand, Krasich [3] used flight data from several interplanetary spacecraft to demonstrate a decreasing failure rate and infant mortality. Although the range of applicability of the previous studies here mentioned is not clearly identified, an obvious disagreement exists with respect to the important matter of satellite failure rate behavior.[1] This is an important matter because the existence of satellite infant mortality will require a different mitigation approach than say wear-out failures. Studies of spacecraft reliability do agree, however, that an exponential lifetime distribution cannot match data from flight experience and that satellite "reliability predictions with MIL-HDBK 217 constant failures rates are unrealistic" [3].

To help resolve this contradiction regarding the existence or not of satellite infant mortality, and by the same token fill the gap in the technical literature with respect to satellite reliability discussed previously, we recently collected failure data for 1584 Earth-orbiting satellites successfully launched between January 1990 and October 2008. We then conducted a nonparametric analysis of satellite reliability and demonstrated that a Weibull distribution with infant mortality (i.e., shape parameter less than one) properly captures the on-orbit failure behavior of satellites [4]. Recall that a Weibull probability density function can be expressed as

$$f(t;\beta,\theta)=\frac{\beta}{\theta}\left(\frac{t}{\theta}\right)^{\beta-1}\exp\left[-\left(\frac{t}{\theta}\right)^{\beta}\right] \quad \text{for } t\geq 0 \tag{1}$$

where β is the shape parameter and θ the scale parameter, both nonnegative. The associated Weibull reliability function is

$$R(t;\beta,\theta)=\exp\left[-\left(\frac{t}{\theta}\right)^{\beta}\right] \tag{2}$$

* Corresponding author. Tel.: +1 404 385 6711; fax: +1 404 894 2760.
E-mail address: jsaleh@gatech.edu (J.H. Saleh).

[1] We are grateful for one reviewer who suggested the following additional references on satellite failure analysis [14–18]. These references discuss satellite infant mortality, however, except for [18], these references may suffer from data obsolescence due to their early publication dates (1970s and 1980s).

0951-8320/$ - see front matter © 2009 Elsevier Ltd. All rights reserved.
doi:10.1016/j.ress.2009.05.004

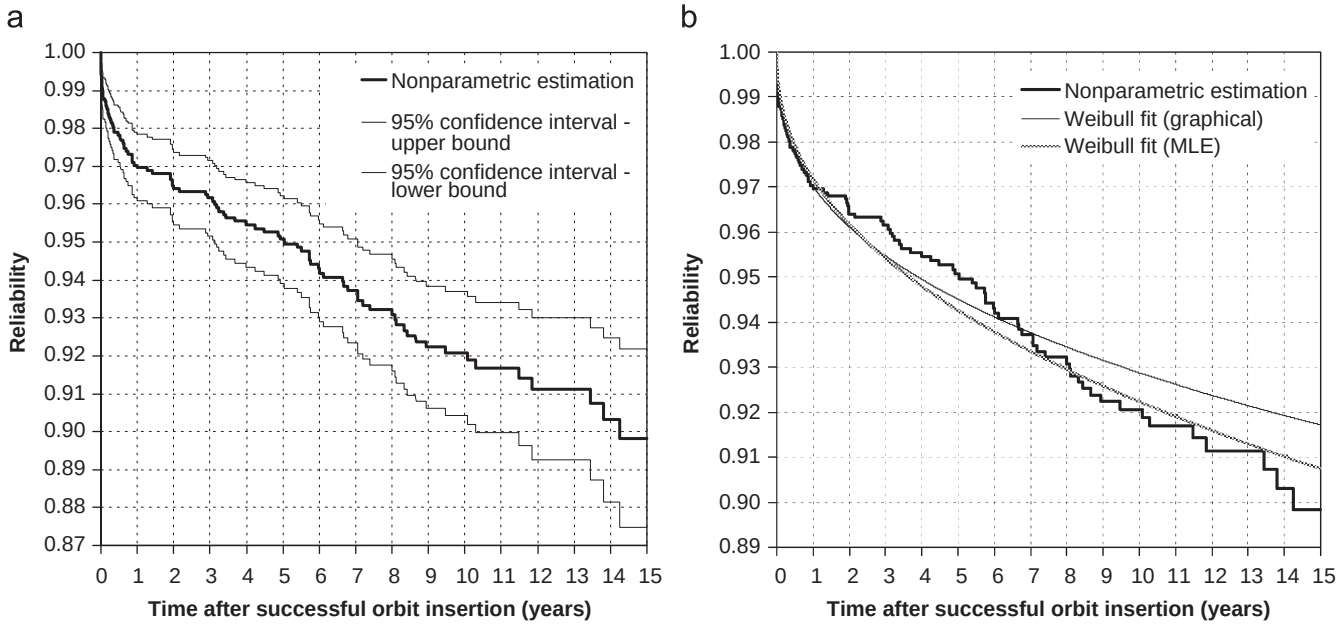

Fig. 1. (a) Satellite reliability with 95% confidence intervals and (b) nonparametric satellite reliability and Weibull fits.

Table 1
Data collection template and sample data for our statistical analysis of satellite reliability (satellites are not arranged/shown in chronological order).

Sample unit number	Launch date	Failure date (if failure occurred)	Culprit subsystem	Censored time (if no failure occurred)
Satellite #1	11/06/1998	11/15/1998	TTC	–
Satellite #2	03/01/2002	–	–	10/02/2008
…	…	…	…	…
Satellite #1584	04/26/2004	03/28/2006	Mechanisms	–

Fig. 1a presents our result for the nonparametric satellite reliability with 95% confidence intervals. Fig. 1b shows the Weibull distribution fitted to this nonparametric reliability with two methods (see Section 4 for details about these methods):

- *Graphical procedure*: The shape parameter of the Weibull fit is $\beta = 0.3875$ and its scale parameter is $\theta = 8316$ years.
- *Maximum likelihood estimation (MLE) procedure*: The shape parameter of the Weibull fit is $\beta = 0.4521$ and its scale parameter is $\theta = 2607$ years.

In this paper, we extend our previous statistical analysis of satellite reliability and investigate satellite subsystems reliability, that is, we further refine our previous analysis from the system-level to the subsystem-level failures. Our objective is to contribute one additional step towards the complete identification of satellite failure mechanisms. In addition to the satellite subsystem reliability, we also conduct a comparative analysis of subsystems failure and identify each subsystem's contribution to satellite failure. In so doing, we identify the "culprit subsystems" that drive satellites unreliability. The results presented in this work should prove useful to the space industry for example in redesigning satellite and subsystem test and screening programs, or providing an empirical basis for subsystem redundancy allocation and reliability growth plans.

The remainder of this paper is organized as follows. In Section 2, we describe the data and the database used in this study. In Section 3, we conduct a nonparametric analysis of satellite subsystems failure. Building on the results of Section 3, we contribute in Section 4 a parametric analysis and Weibull fits of subsystems reliability. Finally, in Section 5, we identify and quantify the relative contribution of each subsystem to the failure of the satellites in our sample. We conclude this work in Section 6.

2. Database and data description

For the purpose of this study, we used the SpaceTrak® database [5]. This database is used by most of the world's launch providers, satellite insurers, satellite operators and manufacturers, and it provides extensive data on satellite on-orbit failure and anomalies, as well as launch histories since 1957. While this database is not "complete" (since some classified satellites for example may not have their failures reported), it is considered the most authoritative database in the space industry with detailed information and failure data for over 6400 spacecraft. More details about this database can be found in [5].

For each spacecraft in our sample, we collect from the database: (1) its launch date; (2) its failure date, if failure occurred; (3) the subsystem identified as having caused the spacecraft failure, hereafter referred to as the "culprit subsystem"; and (4) the "censored time," if no failure occurred. This last point is further explained in the following section where we discuss data censoring and the Kaplan–Meier estimator. The data collection template and sample data for our analysis are shown in Table 1.

Several satellite subsystems are recognized in the database. In this work, we used the following 11 subsystems[2]:

1. Gyro/sensor/reaction wheel (hereafter referred to simply as Gyro)
2. thruster/fuel
3. beam/antenna operation/deployment
4. control processor (CP)
5. mechanisms/structures/thermal (mechanisms)
6. payload instrument/amplifier/on-board data/computer/transponder (payload)
7. battery/cell
8. electrical distribution
9. solar array deployment (SAD)
10. solar array operating (SAO)
11. telemetry, tracking and command (TTC)

For example, a traveling-wave tube (TWT) is categorized under subsystem #6 in the previous list, and the solar array drive, if its failure leads to the non-deployment of the solar arrays, would be categorized under subsystem # 9 in the previous list.

When the culprit subsystem that led to the failure of the satellite could not be identified, the failure of the spacecraft is ascribed to an "unknown" category in the database.

One note is in order regarding the limitation of the present work. While we statistically analyze the "collective" failure behavior of satellites recently launched, it can be argued that no two (or more) satellites are truly alike, and that every satellite operates in a distinct environment (in different orbits or even within the same orbit, where satellites, unless they are co-located, are exposed to different space environment conditions). As a result, the situation of the space industry is very different from that for example of the semi-conductor industry where data on, say, millions of identical transistors operating under identical environmental conditions are available for statistical analysis (or other industries with items for which failure data can be easily obtained from accelerated testing or field operation).

The consequence is that in the absence of "satellite mass production," statistical analysis of satellite/subsystems failure and reliability data faces the dilemma of choosing between calculating precise "average" satellite/subsystems reliability, or deriving a possibly uncertain "specific" satellite/subsystems reliability. This dilemma is explained in the following two possible approaches.

The first approach is to lump together different satellites and analyze their "collective" on-orbit failure behavior (assuming that the failure times of the satellites are independent and identically distributed (iid)). The advantage of doing so is that one can work with a relatively large sample and thus obtain some precision and a narrow confidence interval for the "collective" reliability analyzed. The disadvantage is that the iid assumption may not be realistic, and the "collective" reliability calculated (with precision) may not reflect the specific reliability of a particular type of spacecraft/subsystem.

The second approach is to specialize the data, for example for specific spacecraft platform or mission type, or for satellites in particular orbits. The advantage of doing so is that the reliability analyzed is specific to the type of spacecraft considered (it is no longer a "collective" on-orbit reliability). The disadvantage is that the sample size is reduced, and as a consequence, the confidence interval expands (i.e., the results become increasingly uncertain). Given the available number of satellites (a few thousands), data specialization, which could reduce the sample size to say fewer than a hundred data points, would result in significantly large confidence intervals, and thus highly dispersed or uncertain "specific" satellite/subsystems reliability calculations.

In this paper, we adopt the first approach, that is, we analyze the "collective" failure behavior of Earth-orbiting satellites and subsystems. We discuss the second approach in [6–8] and analyze on-orbit reliability of satellites by mission type, orbit, and mass categories (data for specific satellite platforms and by manufacturer is also available). However, regardless of the choice of the sample, the statistical approach and analysis presented in this paper remains valid.

In the following section, we use the data collected (Table 1) to conduct a nonparametric reliability analysis of all the satellite subsystems identified previously.

3. Nonparametric reliability of satellite subsystems

In this section, we use what is referred in the database as a Class I failure, that is a failure of a subsystem resulting in the retirement of a satellite, to compute the reliability of the considered subsystem.[3] Only the beam/antenna operation/deployment subsystem exhibits no Class I failure in our dataset. Thus, we study the 10 remaining subsystems plus the unknown category.

3.1. Censored data sample and Kaplan–Meier estimator

Censoring occurs when life data for statistical analysis of a set of items is incomplete, which is the case in our sample. More specifically, we have Type IV censoring (also referred to as random censoring), that is right-censoring with staggered entry. This means the following: (1) the satellites in our sample are activated at different points in time (i.e., the satellites are launched at different calendar dates) but all these activation times in our sample are known, (2) failures dates and censoring are stochastic, and (3) censoring occurs either because a satellite is retired from the sample before a failure occurs or because the satellite is still operational at the end of our observation window (October 2008). In addition, when analyzing failure due to a particular subsystem, a failure due to any other subsystem constitutes an additional form of censoring. Censoring requires careful attention: deriving a reliability function from censored life data is not trivial, and it is important that it is done properly if the results are to be meaningful and unbiased. In this work, we adopt the powerful Kaplan–Meier estimator [9], which is best suited for handling the type of censoring we have in our sample. The derivation of the Kaplan–Meier estimator formula can be found in [4]. The Kaplan–Meier estimator of the reliability function with censored

[2] These categories are not necessarily spacecraft "subsystems" in the traditional meaning of the word. For example, the "battery/cell" and "electrical distribution" are part of the spacecraft "power subsystem" but they are clearly identified in the database when they cause a spacecraft failure. As a result, we have in some of these categories a finer resolution for causes of spacecraft failure than the subsystem level (i.e., in some cases, it is the failure at the sub-subsystem level that is identified). Notice also that the "solar array deployment" is a one-shot "subsystem" or more precisely, a one-shot phase of the solar array sub-subsystem. For convenience, we refer to all these 11 items in the list as "subsystems."

[3] It should be noted that this is a slightly modified version of the traditional definition of "unreliability" where the failure of an item, here a subsystem, is accounted for when it leads to a failure of the system in which it is embedded. In essence, this implies that all these subsystems are indispensable for the successful operation of the satellite, and in a reliability block diagram, these subsystems/functions are placed in series. Partial subsystem failures will be discussed and analyzed in a follow-up work.

data is given by

$$\hat{R}(t) = \prod_{\text{all } i \text{ such that } t_{(i)} \le t} \hat{p}_i = \prod_{\text{all } i \text{ such that } t_{(i)} \le t} \frac{n_i - 1}{n_i} \tag{3}$$

where

$$\begin{cases} t_{(i)}: \text{ time to } i\text{th failure (arranged in ascending order)} \\ \hat{p}_i = \frac{n_i - 1}{n_i} \\ n_i = \text{number of operational units right before } t_{(i)} \\ \quad = n - [\text{number of censored units right before } t_{(i)}] \\ \quad\quad - [\text{number of failed units right before } t_{(i)}] \end{cases} \tag{4}$$

Should there be ties in the failure times, say m_i units failing at exactly $t_{(i)}$—this situation is referred to as a tie of multiplicity m—then Eq. (4) is replaced by

$$\hat{p}_i = \frac{n_i - m_i}{n_i} \tag{5}$$

If a censoring time is exactly equal to a failure time, a convention is adopted that assumes censoring has occurred immediately after the failure (that is, at an infinitely small time interval after the failure).

3.2. Confidence interval analysis

The Kaplan–Meier estimator (Eq. (3)) provides a maximum likelihood estimate of reliability but does not inform us about the dispersion around $\hat{R}(t_i)$. This dispersion is captured by the variance or standard deviation of the estimator, which is then used to derive the upper and lower bounds for say a 95% confidence interval (that is, a 95% likelihood that the actual reliability will fall between the two calculated bounds, with the Kaplan–Meier analysis providing us with the most likely estimate). The variance of the estimator is provided by Greenwood's formula:

$$\hat{var}[R(t_i)] \equiv \sigma^2(t_i) = [\hat{R}(t_i)]^2 \sum_{j \le i} \frac{m_j}{n_j(n_j - m_j)} \tag{6}$$

And the 95% confidence interval is determined by

$$R_{95\%}(t_i) = \hat{R}(t_i) \pm 1.96\sigma(t_i) \tag{7}$$

More details about these equations can be found in [10–12].

3.3. Kaplan plots of satellite subsystems reliability

With this brief overview of censoring, of the Kaplan–Meier estimator, and of confidence intervals, we can now analyze the on-orbit satellite subsystems reliability from our censored data sets (one for each subsystem). For the 1584 satellites analyzed, and the 11 subsystems considered, we obtained 17,424 censored and failure times. For reading convenience and space, this data is not included here but it can be made available from the authors upon request. The data is treated with the Kaplan–Meier estimator (Eq. (3)), and we obtain the Kaplan–Meier plots of the reliabilities of all the satellite subsystems listed in Section 2. In addition, when Eqs. (6) and (7) are applied to the data from our sample, we obtain the 95% confidence interval curves. The Kaplan plots of the reliabilities of all the satellite subsystems here considered along with the 95% confidence intervals are shown in Figs. 2a and b.

Figs. 2a and b read as follows. Consider the Gyro/sensor/reaction wheel subsystem, its reliability is shown in the upper-left corner of Fig. 2a: after a successful launch, the reliability of the Gyro/sensor/reaction wheel subsystem drops to approximately 99.5% after 4 years on-orbit. More precisely, we have

$$\hat{R}(t) = 0.9948 \quad \text{for } 1146 \text{ days} \le t < 1967 \text{ days} \quad \text{that is } 3.137 \text{ years} \le t < 5.385 \text{ years}$$

In addition, the reliability of this subsystem will fall between 99.09% and 99.86% with a 95% likelihood (confidence interval) over this period of time. This same "reading grid" of Figs. 2a and b regarding the estimated reliability $\hat{R}(t)$ and confidence interval applies to all the other subsystems. For example, the reliability of the TTC subsystem (lower-right corner of Fig. 2b) drops to 0.984 after 8 years on-orbit. Notice the particular nonparametric reliability of the solar array deployment (a constant), which is due to the one-shot nature of this "subsystem" (or more precisely, this phase of the solar array subsystem). In the next section, we provide a Weibull parametric fit for each of these subsystems' nonparametric reliability results.

4. Parametric reliability of satellite subsystems

Nonparametric analysis provides powerful results since the reliability calculation is unconstrained to fit any particular pre-defined lifetime distribution. However, this flexibility makes nonparametric results neither easy nor convenient to use for various purposes often encountered in engineering design (e.g., reliability-based design optimization). In addition, some failure trends and patterns are more clearly identified and recognizable with parametric analysis. Several possible methods are available to fit a parametric distribution to the nonparametric estimated reliability function (as provided by the Kaplan–Meier estimator), such as graphical procedures and inference procedures. In the following, we briefly review two such methods, the probability plots and the maximum likelihood estimation; we use the former to justify our choice of a Weibull distribution for modeling satellite subsystem reliability and the latter to calculate the parameters of each Weibull distribution.

4.1. Probability plots or graphical estimation

We begin our review of fitting techniques with the easy-to-use and visually appealing graphical technique known as probability plotting (or plotting positions). We use this technique to demonstrate that the Weibull distribution is an appropriate choice for capturing the failure behavior of satellites and satellite subsystems.

Probability plots constitute a simple graphical procedure for fitting a parametric distribution to nonparametric data. This procedure is based on the fact that some parametric models, such as the exponential or Weibull distribution for example, can have their reliability function linearized using a particular mathematical transformation. Consider for example the Weibull distribution. By taking the natural logarithm of both sides of Eq. (2), we obtain

$$\ln[R(t)] = -\left(\frac{t}{\theta}\right)^{\beta} \tag{8}$$

Taking again the natural logarithm of the (negative of the) two sides of this equality, we obtain:

$$\ln[-\ln R(t)] = \beta \ln(t) - \beta \ln(\theta) \tag{9}$$

Eq. (9) is equivalent to Eq. (2)

$$R(t) = \exp\left[-\left(\frac{t}{\theta}\right)^{\beta}\right] \Leftrightarrow \ln[-\ln R(t)] = \beta \ln(t) - \beta \ln(\theta) \tag{10}$$

Now assume that we do not know the underlying parametric distribution, but we have the nonparametric reliability estimate for an item, $\hat{R}(t_i)$, at different points in time t_i. If we plot $\ln[-\ln \hat{R}(t_i)]$ as a function of $\ln(t_i)$ and we obtain data points that are aligned in the $(\ln(t);\ \ln[-\ln \hat{R}(t)])$ space—the resulting graph is termed the Weibull plot—then we can conclude that the data effectively arise from a Weibull distribution (i.e., the underlying parametric distribution is indeed a Weibull). In addition, the slope of the line that fits these data points provides us with shape parameter β of the Weibull distribution. And the scale parameter θ can be evaluated for example from the value of the intersection of the line with the y-axis.

Parametric distributions other than the Weibull also have their corresponding "probability plots" (e.g., exponential, normal or lognormal probability plots), and if the discrete nonparametric data calculated are aligned on these probability plots, then it can be concluded that the data effectively arise from the associated distribution.

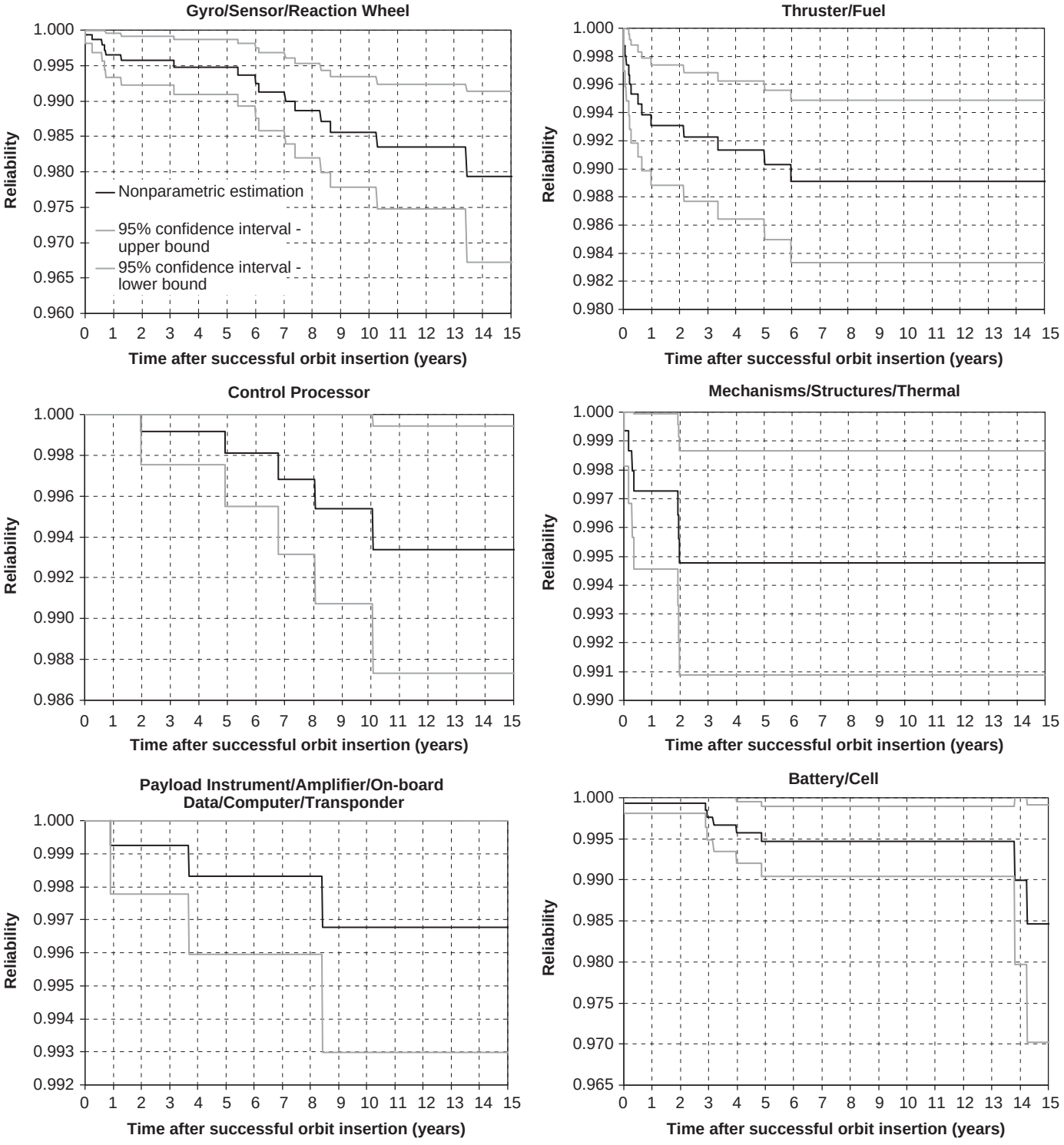

Fig. 2. (a) and (b) Satellite subsystems reliability with 95% confidence intervals.

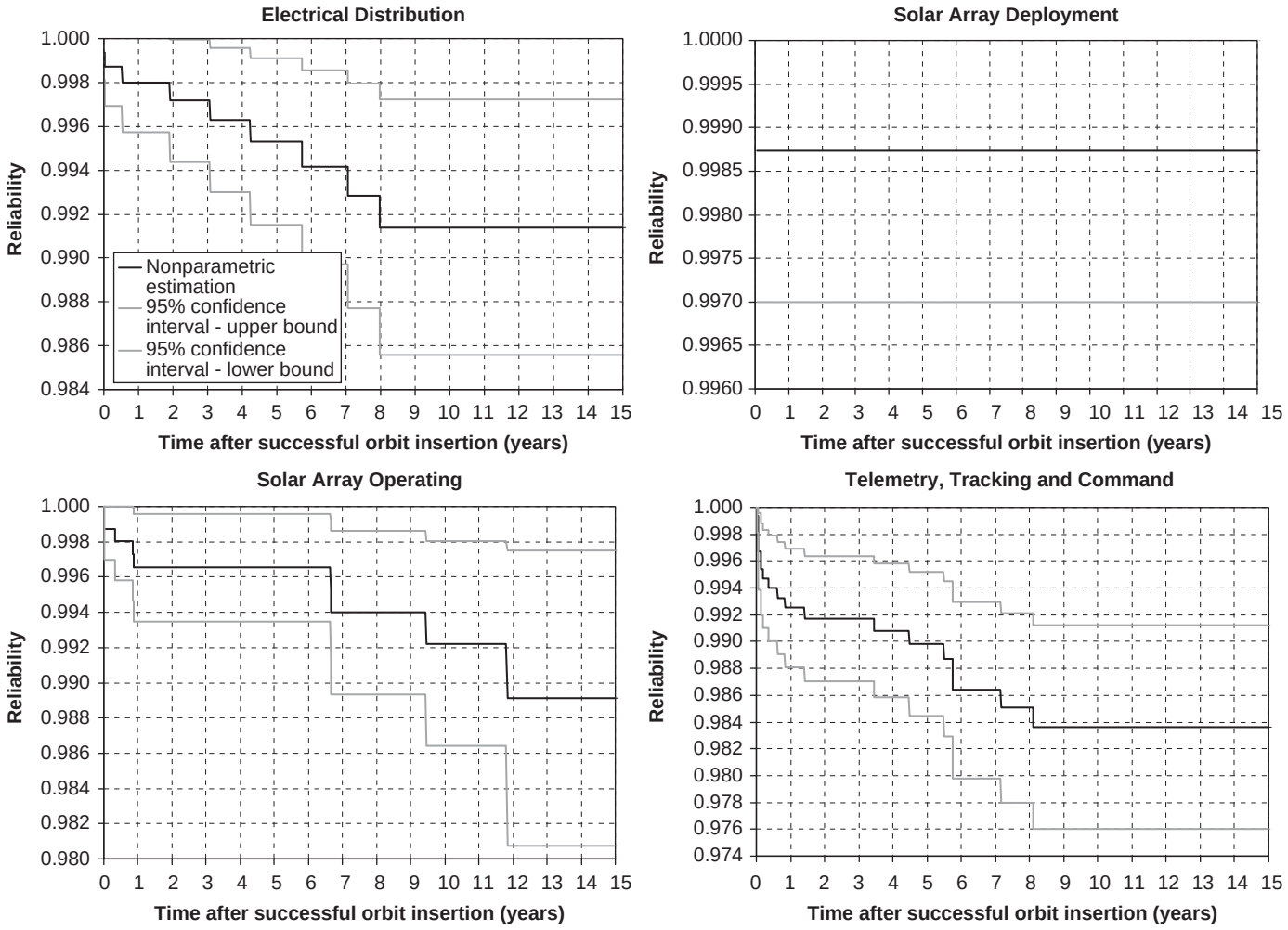

Fig. 2. (*Continued*)

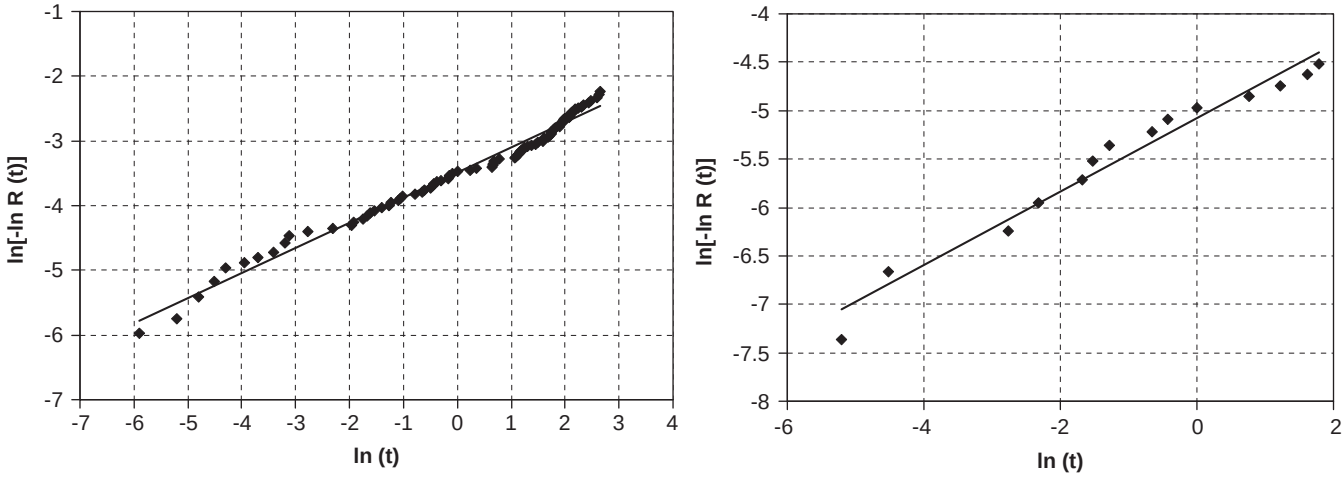

Fig. 3. Weibull plots of satellite (left) and thruster/fuel subsystem (right) reliability (shown above are the data points and linear least-squares fit).

We restrict ourselves in the present work to Weibull plots (notice that if the underlying distribution is an Exponential, it can be easily identified on the Weibull plot when the slope of the line, which corresponds to the shape parameter, is equal to one). Fig. 3 shows the Weibull plots for satellite reliability and the thruster/fuel subsystem reliability.

The data points in Fig. 3 are well aligned thus providing a good indication that the Weibull fit is indeed a good one for both the

satellite reliability and the thruster/fuel subsystem reliability.[4] Similar results are obtained for the other subsystems. We can therefore state that satellite reliability and satellite subsystems reliability (with the exception of the solar array deployment) can be properly approximated by Weibull distributions. We discuss the goodness-of-fit of this distribution later in this section.

Probability plots or graphical methods for parametric fit have a powerful advantage in their simplicity: they are easy to set up, they do not require involved calculations, and they give immediate (visual) information about the validity (or not) of the assumed parametric distribution. In addition, the parameters of the assumed distribution (in our case the Weibull distribution) can be calculated by simple least-square linear fit of the data on the probability plots. However, probability plots have some disadvantages when used to calculate the actual parameters of the distribution. For example,

(i) With distributions requiring logarithm time transformations (e.g., Weibull or lognormal distribution), excessive weight is given to the early failure times, and as a consequence, the resulting parametric fit is biased (towards more precision for early failures).
(ii) As a consequence of (i), the least-square fit on the probability plot does not result in minimum variance estimate of the actual distribution.
(iii) The estimation of the parameters may be poor if the failure times are not scattered properly across the data range.

If the purpose or objectives of conducting the reliability study do not require "precise" results, then probability plots or graphical estimations are adequate for conducting parametric fits. Otherwise, one can revert to the more precise, but analytically involved, maximum likelihood estimation method, discussed next. For the purpose of this work, we used probability plots to justify our choice of a Weibull distribution for modeling satellite subsystem reliability, then we used MLE to calculate the parameters of the Weibull distributions.

4.2. Maximum likelihood estimation

Maximum likelihood estimation addresses all the limitations of probability plots and provides more precise parametric fits than graphical estimation.[5] While conceptually simple, the MLE method is analytically involved and requires, (1) determining the right formulation of a function (known as the likelihood function) depending on several parameters (e.g., censoring type, chosen parametric distribution), and (2) searching for an optimum of this function, which can prove analytically tedious by calculating a set of partial derivatives of the logarithm of the likelihood function, and/or numerically intense by non-linear optimization techniques. In the following, we provide a brief overview of this method. The reader interested in more details is referred to [13].

Conceptually, MLE is based on the following: given a set of observed data, and assuming a parametric life distribution with unknown parameters (e.g., two parameters for the Weibull distribution), a likelihood function is defined as the probability of obtaining/generating the observed data from the chosen parametric distribution. When an exhaustive search is conducted over the unknown parameters of the distribution, the values of these parameters that maximize the likelihood function are termed the maximum likelihood estimates and the methods is known as the MLE. The analytical derivation of the MLE is provided in Appendix.

[4] The linear least-square fit has a coefficient of determination $R^2 = 0.9835$ and 0.9670 for the satellite and the thruster/fuel subsystem, respectively.

[5] As long as the sample size is not exceedingly small (e.g., in the single digits).

Table 2
Maximum likelihood estimates of the Weibull parameters for subsystems reliability.

Subsystem	β	θ (years)
Gyro/sensor/reaction wheel	0.7182	3831
Thruster/fuel	0.3375	6,206,945
Control processor	1.4560	408
Mechanisms/structures/thermal	0.3560	21,308,746
Payload instrument/amplifier/on-board Data/computer/ transponder	0.8874	7983
Battery/cell	0.7460	7733
Electrical distribution	0.5021	169,272
Solar array deployment	–	–
Solar array operating	0.4035	1,965,868
Telemetry tracking and command	0.3939	400,982

Table 3
Error between the nonparametric and Weibull reliability for each subsystem.

Subsystem	Maximum error	Average error
	Percentage point	
Gyro/sensor/reaction wheel	0.37	0.14
Thruster/fuel	0.18	0.08
Control processor	0.22	0.06
Mechanisms/structures/thermal	0.21	0.07
Payload instrument/amplifier/on-board data/computer/ transponder	0.36	0.27
Battery/cell	0.62	0.15
Electrical distribution	0.19	0.07
Solar array deployment	–	–
Solar array operating	0.31	0.13
Telemetry tracking and command	0.23	0.10

4.3. MLEs of Weibull satellite subsystems reliability parameters

Having shown that the Weibull distribution is indeed a good fit for the reliability of satellite subsystems, we next apply the MLE procedure with a second-order gradient-based method to determine the Weibull parameter estimates for each subsystem. The results are provided in Table 2.

The information in Table 2 reads as follows. Consider for example the Gyro subsystem. Its nonparametric reliability is best approximated by the following Weibull distribution:

$$R_{Gyro}(t) = \exp\left[-\left(\frac{t}{3831}\right)^{0.7182}\right] \tag{11}$$

The values of the shape parameter ($\beta = 0.7182$) and the scale parameter ($\theta = 3831$) are the maximum likelihood estimates.

Note that no values of the Weibull parameters are provided for the solar array deployment subsystem. Indeed, as discussed previously and seen in Fig. 2b, the "solar array deployment" is a one-shot "subsystem" or more precisely, a one-shot phase of the solar array sub-subsystem and a Weibull fit is not meaningful in this case. A Weibull fit can also be conducted on the data assigned to the "unknown" category mentioned in Section 2. The resulting Weibull parameters are $\beta = 0.4011$ and $\theta = 5{,}836{,}474$ years.

The important result in Table 2 is that all satellite subsystems, with the exception of the control processor, suffer from infant mortality (shape parameter $\beta < 1$). This finding has important implications for the space industry and should prompt serious

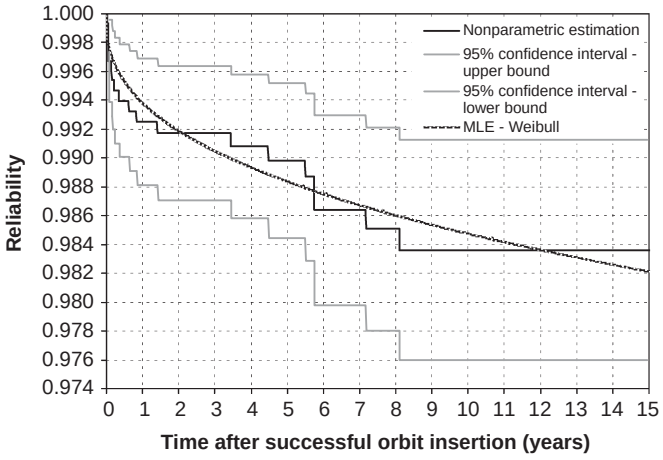

Fig. 4. Nonparametric reliability and Weibull fit for the TTC subsystem.

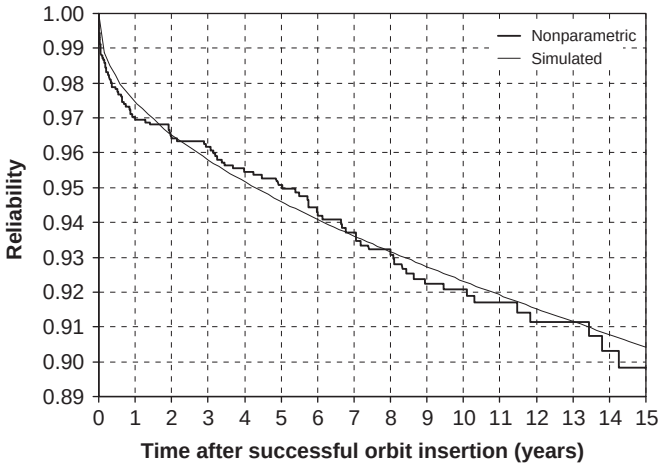

Fig. 5. Comparison between nonparametric and simulated satellite reliability.

consideration for improved subsystem testing and burn-in procedures.

Fig. 4 shows the nonparametric reliability curve (with the 95% confidence interval) for the TTC subsystem, as well as the best Weibull fit (i.e., with MLE parameters).

Fig. 4 provides a visual verification that the Weibull distribution with the MLE parameters provided in Table 2 is a good fit for the TTC nonparametric reliability. Similar results are obtained for the other subsystems. The goodness-of-fit of the Weibull distribution is simply reflected in this work by the maximum and average errors over 15 years between the nonparametric reliability curve and the Weibull fit.[6] For example, for the TTC subsystem, the maximum error (or distance) between the nonparametric reliability curve and the Weibull fit is 0.23 percentage point, and the average error is 0.10 percentage point. This represents a remarkable accuracy for a two-parameter (Weibull) distribution.

It should be pointed out that more accurate models of the nonparametric subsystems reliability can be developed—if more accuracy is needed—by adopting either spline functions or a mixed model distribution with more parameters (hence more degrees of freedom) than the two-parameter Weibull distribution or other traditional parametric distributions. More complex models for satellite subsystem reliability will be investigated in future work.

Table 3 provides the maximum and average error between the nonparametric reliability and the Weibull fit for all the subsystems. The maximum error for all the subsystems remains smaller than one percentage point (the worst fit being for the battery/cell with a maximum error of 0.62 percentage point). These results indicate that the Weibull distribution is a reasonably accurate model for the reliability of all the subsystems (with the exception of the solar array deployment).

4.4. Verification of the MLE results

To verify our results for the reliability of subsystems obtained through the MLE method, we adopted two approaches. First, we conducted a (brute force) non-linear least-square estimate directly on the nonparametric data. The results were found to be significantly close to the ones obtained with the MLE method. Second, more importantly, we simulated the parametric reliability of all the subsystems and compared it with the satellite nonparametric reliability. Recall that our subsystem reliability calculations are based on the definition of Class I failure in SpaceTrak®, that is a failure of a subsystem that results in the retirement of a satellite. Given that the database ascribes the cause of the satellite failure to a single subsystem (or the "unknown" category), the subsystems are therefore considered in series with respect to Class I failure. In other words, the failure of any subsystem leads to the failure of the satellite (by definition of the Class I failure). We therefore ran Monte Carlo simulation of all the subsystems in series with their corresponding Weibull distributions. The resulting "simulated" satellite reliability was compared to the actual nonparametric satellite reliability. The result is shown in Fig. 5.

The "simulated" satellite reliability based on the aggregate Weibull subsystems reliability derived in this work follows remarkably well the nonparametric satellite reliability. The error between the two curves remains within less than one percentage point. This is a good indication that the subsystems reliability derived in this work using the MLE method are indeed appropriate.

5. Relative contribution of each subsystem to satellite failure

In this section, we provide a comparative analysis of subsystem failure and identify the culprit subsystems driving satellite unreliability. More specifically, we quantify the relative contribution of each subsystem to the failure of the satellites in our sample. In addition, we add a time dimension to this analysis by analyzing the evolution over time of the relative contribution of each subsystem to the satellite loss.

For each subsystem j identified in our database, we calculate its probability of leading to the failure of the satellite, $\hat{P}_{subsystem,j}$, based on the estimated reliability of the subsystem obtained by the Kaplan–Meier estimator on Section 2:

$$\hat{P}_{subsystem,j} = 1 - \hat{R}_{subsystem,j} \tag{12}$$

We then compute the probability of failure of a satellite as follows:

$$\hat{P}_{satellite} = 1 - \hat{R}_{satellite} \tag{13}$$

where $\hat{R}_{satellite}$ is the estimated nonparametric satellite reliability obtained with the Kaplan–Meier estimator (shown in Fig. 1).

[6] Formal goodness-of-fit tests are beyond the scope of this work and their contributions to our findings (beyond the Weibull plots) are marginal.

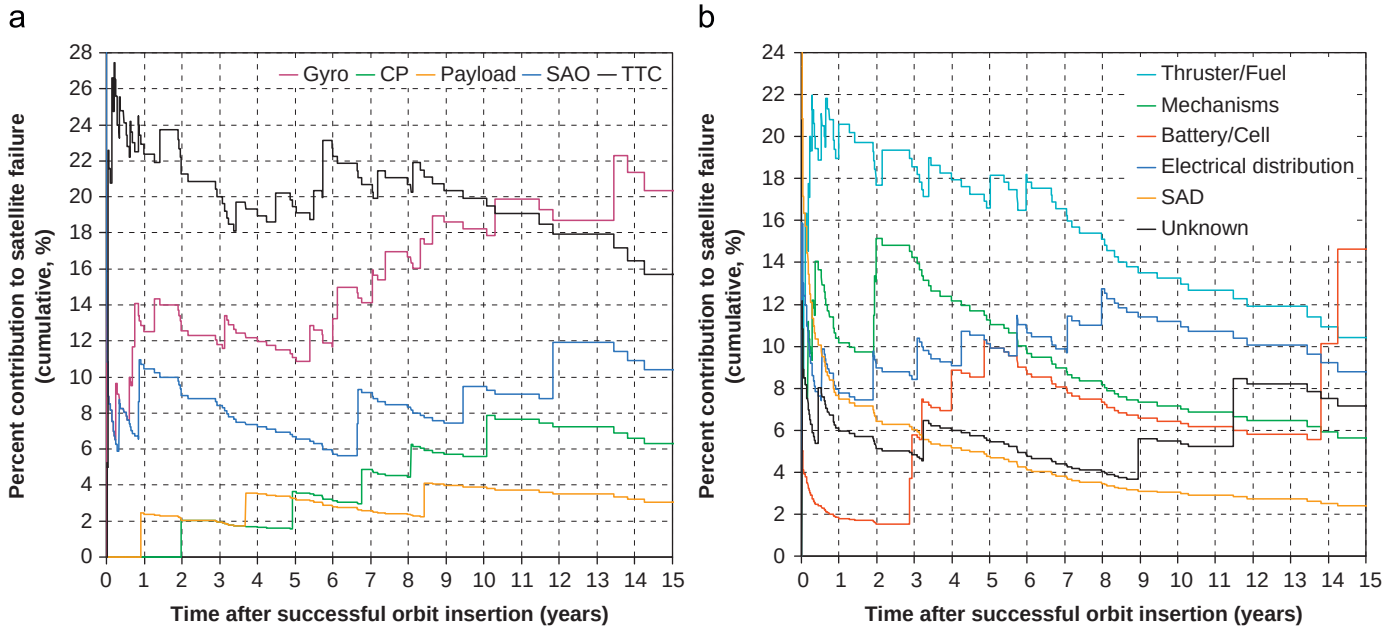

Fig. 6. (a) (left) and (b) (right). Relative contributions of various subsystems to satellite failure.

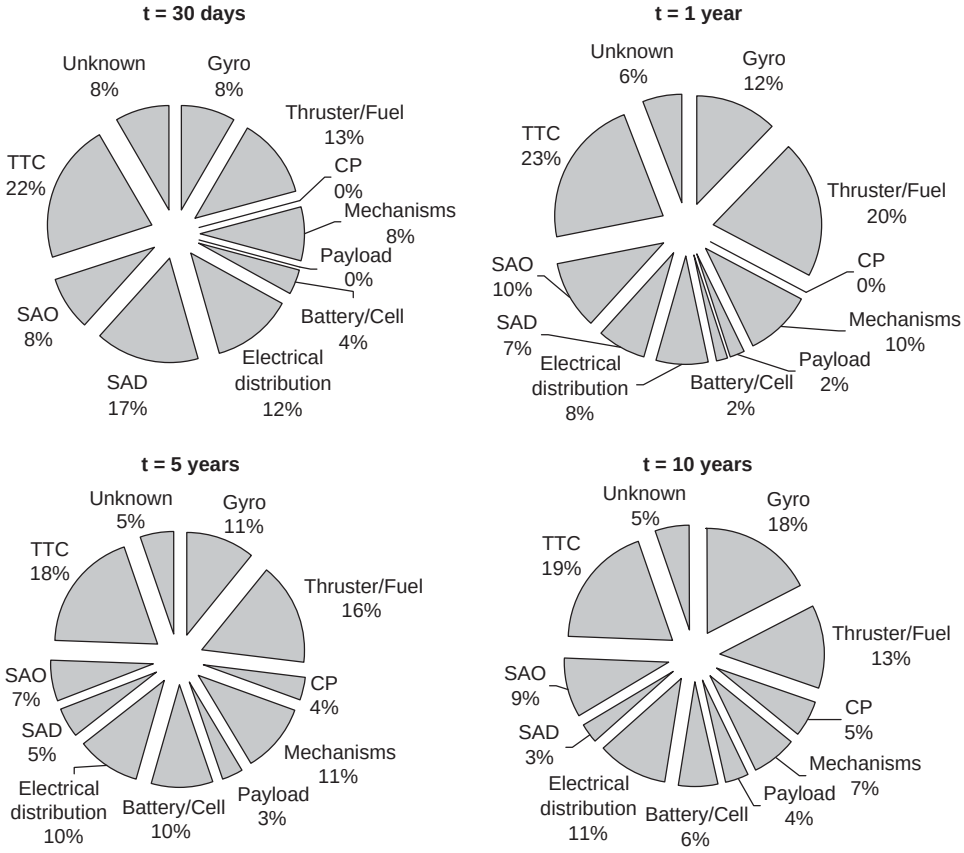

Fig. 7. Subsystem contributions to satellite failures after 30 days, 1 year, 5 years, and 10 years on-orbit.

The percentage contribution of subsystem j to the failure of a satellite is then given by

$$r_j = \frac{\hat{P}_{subsystem,j}}{\hat{P}_{satellite}} \tag{14}$$

The results of our analysis can be represented in one figure, showing all the r_j for $j = 1$–11 as a function of time. However, for readability purposes, we have split the results into three figures: Figs. 6a, b and 7.

Figs. 6a and b show the evolution over time of the distribution of subsystems failures leading to the loss of the satellite. For

example, in Fig. 6a, we see that the control processor contributes approximately 6% to the total failures of satellite over 15 years. Similarly, we observe that the Gyro and TTC are the major contributors to satellite failures with, respectively, 20% and 16% of satellite failures due to these subsystems over a period of 15 years.

It is interesting to note the switch in "failure leadership" between the Gyro and TTC subsystems around year 10 on Fig. 6a. The TTC is the lead contributor to satellite failure over the first 10 years on-orbit, with a relative contribution hovering around 20%. The failures due to the Gyro remain around 12% between year 1 and year 6 on-orbit, and then they clearly ramp up starting around year 6 and overtake the relative contributions of the TTC subsystem to satellite failure. We term this occurrence the switch in "failure leadership" between the Gyro and TTC subsystems.

Fig. 6b shows, for example, that unknown causes account for 5–8% of satellite failures. One interesting trend on Fig. 6b is the evolution of the battery contribution to satellite failure. We observe two clear increases in $r_{battery}$: the first one around year 3 on-orbit when satellite failures due to batteries ramp up from 2% to 10% by year 5; and the second one around year 14 when satellite failures due to batteries ramp up from 6% to 14% by year 15 (this information can also be seen in Fig. 2a). These observations are likely indicative of two different failure modes, and as such, they should be useful to electrical engineers working on spacecraft power storage and the corresponding reliability testing program.

Fig. 7 provides a more readable version of Figs. 6a and b. Instead of the evolution over time of r_j, Fig. 7 provides a snapshot or static picture of the subsystems' contribution to satellite failures at four discrete points in time, after 30 days, after 1 year, after 5 years, and after 10 years on-orbit. Fig. 7 in effect represents vertical cuts across Figs. 6a and b, and while we lose the dynamical information portrayed in these figures, we gain in readability and accuracy (or finer resolution) at the discrete points in time selected.

The observations made in Figs. 6a and b can be found in Fig. 7. In addition, notice in the upper-left quadrant of Fig. 7 that the solar array deployment and TTC account, respectively, for 17% and 22% of the failures of the first 30 days on-orbit. Thus satellite infant mortality, as discussed in [4], is driven to a large extent by these two subsystems.

The analysis in this section should prove useful to the space industry in general, and satellite designers and program managers in particular in helping them focus their attention and resources on subsystems with high(er) propensity for and contribution to satellite failure, thus improving subsystem test and screening programs.

6. Conclusion

Reliability has long been recognized as a critical design attribute for space systems. Spacecraft are high-value assets whose cost often exceeds hundred of millions of dollars and whose "location" or operational environment renders them physically inaccessible for maintenance to compensate for sub-standard reliability. Despite these observations, limited on-orbit data and statistical analyses of spacecraft reliability exist in the technical literature. In this work, we filled this gap by conducting nonparametric statistical analysis of satellite reliability and satellite subsystems reliability. We demonstrated that the Weibull distribution is a good fit for subsystem reliability and calculated the Weibull parameters using the maximum likelihood estimation technique. One important result from our parametric analyses is that all satellite subsystems, with the exception of the control processor, exhibit infant mortality. This finding has important implications for the space industry and should prompt serious consideration for improved subsystem testing and burn-in procedures.

Finally, we quantified the relative contribution of each subsystem to the failure of satellites and identified the subsystems that drive satellite unreliability. For example, we found that the Gyro and TTC subsystems are major contributors to satellite failures, and the TTC and solar array deployment drive satellite infant mortality.

In forthcoming work, we further extend the exploration of failure mechanisms of satellites and satellite subsystems by conducting, beyond the "binary" concept of reliability (an item is considered either operational or failed), a multi-state failure analysis with degraded states in subsystems functionality.

Acknowledgements

This work was funded in part by a grant from Orbital Sciences Corporation/DARPA from the F6 Fractionated Spacecraft Program. The support is gratefully acknowledged.

Appendix. Derivation of the maximum likelihood estimates

The following maximum likelihood estimation derivation is based on Lawless [13]. Suppose that the potentially observable data in a study is distributed according a probability distribution defined by the parameter vector $\boldsymbol{\theta}$. Then, calling Data the data actually observed, the likelihood function for $\boldsymbol{\theta}$ based on these data is

$$L(\boldsymbol{\theta}) = Pr(\text{Data};\boldsymbol{\theta}) \tag{15}$$

where Pr represents the probability density or mass function from which the observed data are assumed to arise. When the probability density function has a parametric form $f(t;\boldsymbol{\theta})$, and the independent and identically distributed lifetimes $t_1,\ldots,t_n$ for a random sample of n individuals are observed, Eq. (15) can be rewritten as

$$L(\boldsymbol{\theta}) = \prod_{i=1}^{n} f(t_i;\boldsymbol{\theta}) \tag{16}$$

This function can be maximized to obtain an estimate $\widehat{\boldsymbol{\theta}}$ and an estimate of the reliability function $R(t;\widehat{\boldsymbol{\theta}})$ according to the probability distribution.

Difficulty arises when the data is censored: Eq. (16) cannot be used anymore and a probability model for the censoring mechanism is needed. As before, let us consider n individuals having the following lifetimes $t_1,\ldots,t_n$. Let us introduce the variable δ_i accounting for the censoring in the data: if t_i is an observed lifetime, $\delta_i = 1$; if t_i is a censoring time, $\delta_i = 0$. Then, for most of the censoring mechanisms, and for the censoring type we are facing in our study, the likelihood function in the continuous case can be written when all lifetimes and censoring times are independent as

$$L(\boldsymbol{\theta}) = \prod_{i=1}^{n} f(t_i;\boldsymbol{\theta})^{\delta_i} R(t_i;\boldsymbol{\theta})^{1-\delta_i} \tag{17}$$

where $f(t;\boldsymbol{\theta})$ and $R(t;\boldsymbol{\theta})$ are, respectively, the probability density function and the reliability function of the probability distribution from which the data is assumed to arise.

One of the difficulties associated to the MLE, as expressed in the previous subsection, comes from the fact that the likelihood function needs to be derived specifically for each parametric distribution. We are interested in this paper in the Weibull distribution as expressed in Eqs. (1) and (2). Instead of working directly with Eqs. (1) and (2), it can be more convenient to work

with the equivalent extreme value distribution for $Y = \log T$, with the following p.d.f. and reliability function:

$$f(y;u,b) = \frac{1}{b} e^{(y-u)/b} \exp[-e^{(y-u)/b}], \quad -\infty < y < \infty \tag{18}$$

$$R(y;u,b) = \exp[-e^{(y-u)/b}], \quad -\infty < y < \infty \tag{19}$$

where $y = \log t$, $u = \log \theta$ and $b = \beta^{-1}$.

As the maximization process is unchanged by monotonic transformation, it is usually more convenient to use the log-likelihood function $l(\boldsymbol{\theta}) = \log L(\boldsymbol{\theta})$. By using the change of variables $z = (y-u)/b$, and introducing $r = \sum \delta_i$, the log-likelihood function is expressed as

$$l(u,b) = -r \log b + \sum_{i=1}^{n} (\delta_i z_i - e^{z_i}) \tag{20}$$

We can now maximize the log-likelihood function $l(u,b)$, or minimize $-l(u,b)$, which is the case retained in this study. To make the minimization problem more efficient, we can also compute the gradient and the Hessian of $-l(u,b)$, which have an analytical and rather simple form:

$$-\nabla l(u,b) = \begin{pmatrix} -\frac{\partial l}{\partial u} \\ -\frac{\partial l}{\partial b} \end{pmatrix} = \begin{pmatrix} \frac{1}{b}\sum_{i=1}^{n}[\delta_i - e^{z_i}] \\ \frac{r}{b} + \frac{1}{b}\sum_{i=1}^{n} z_i(\delta_i - e^{z_i}) \end{pmatrix} \tag{21}$$

$$-H(u,b) = \begin{bmatrix} -\frac{\partial^2 l}{\partial u^2} & -\frac{\partial^2 l}{\partial u \partial b} \\ -\frac{\partial^2 l}{\partial u \partial b} & -\frac{\partial^2 l}{\partial b^2} \end{bmatrix} \tag{22}$$

where

$$-\frac{\partial^2 l}{\partial u^2} = \frac{1}{b}\sum_{i=1}^{n} e^{z_i} \tag{23}$$

$$-\frac{\partial^2 l}{\partial u \partial b} = \frac{1}{b^2}\sum_{i=1}^{n}[e^{z_i} - \delta_i + z_i e^{z_i}] \tag{24}$$

$$-\frac{\partial^2 l}{\partial b^2} = \frac{1}{b^2}\left[-r + \sum_{i=1}^{n}[2z_i(e^{z_i} - \delta_i) + z_i^2 e^{z_i}]\right] \tag{25}$$

References

[1] Dezelan RW. Mission sensor reliability requirements for advanced GOES spacecraft. Aerospace report no. ATR-2000(2332)-2, 1999.

[2] Brown O, Long A, Shah N, Eremenko P. System lifecycle cost under uncertainty as a design metric encompassing the value of architectural flexibility. In: AIAA-2007-6023, AIAA SPACE 2007 conference and exposition, Long Beach, CA, September 18–20, 2007.

[3] Krasich M. Reliability prediction using flight experience: Weibull adjusted probability of survival method. NASA technical report, Jet Propulsion Laboratory, Document ID: 20060041898, April 1995.

[4] Castet J-F, Saleh JH. Satellite reliability: statistical data analysis and modeling. Journal of Spacecraft and Rockets, 2009, accepted.

[5] Ascend SpaceTrak® [online database], URL: http://www.ascendworldwide.-com/spacetrak.aspx [cited 24 February 2009].

[6] Castet J-F, Saleh JH. Geosynchronous communication satellite reliability: statistical data analysis and modeling. In: 27th AIAA International Communications Satellite Systems Conference (ICSSC 2009), Edinburgh, Scotland, 1–4 June 2009.

[7] Hiriart T, Castet J-F, Lafleur JM, Saleh JH. Comparative reliability of GEO, MEO, LEO and eccentric Earth-orbiting satellites. In: 60th international astronautical congress, Daejeon, Republic of Korea, 12–16 October 2009.

[8] Dubos GF, Castet J-F, Saleh JH. Statistical data analysis of satellite reliability with covariate: does (spacecraft) size matter? In: 60th international astronautical congress, Daejeon, Republic of Korea, 12–16 October 2009.

[9] Kaplan EL, Meier P. Nonparametric estimation from incomplete observations. Journal of the American Statistical Association 1958;53(282): 457–81.

[10] Ansell JI, Phillips MJ. Practical methods for reliability data analysis. Oxford: Clarendon Press; 1994.

[11] Meeker WO, Escobar LA. Statistical methods for reliability data. New York: Wiley; 1998.

[12] Rausand M, Høyland A. System reliability theory: models, statistical methods, and applications. 2nd ed. New Jersey: Wiley-Interscience; 2004.

[13] Lawless JF. Statistical models and methods for lifetime data. 2nd ed. New York: Wiley; 2003.

[14] Timmins, AR. A study of 1st-month spacecraft malfunctions. NASA technical report TN D-7750, 1974.

[15] Norris, HP, Timmins, AR. Failure rate analysis of Goddard Space Flight Center spacecraft performance during orbital life. In: Proceedings of the annual reliability and maintainability symposium, Las Vegas, NV, 20–22 January 1976.

[16] Baker JC, Baker GA. Impact of space environment on spacecraft lifetimes. Journal of Spacecraft and Rockets 1980;17(5):479–80.

[17] Hecht H, Fiorentino, E. Reliability assessment of spacecraft electronics. In: Proceedings of the annual reliability and maintainability symposium, Philadelphia, PA, 27–29 January 1987.

[18] Sperber, R. Better with age and experience—observed satellite in-orbit anomaly rates. AIAA-1994-1083. In: 15th AIAA international communications satellite systems conference, San Diego, CA, 28 February–3 March 1994.